Hydrogen storage in BC_3 composite single-walled nanotube: a combined density functional theory and Monte Carlo investigation*

Liu Xiu-Ying(刘秀英)[a)b)†], Wang Chao-Yang(王朝阳)[b)], Tang Yong-Jian(唐永建)[b)], Sun Wei-Guo(孙卫国)[c)], and Wu Wei-Dong (吴卫东)[b)]

[a)] *College of Science, Henan University of Technology, Zhengzhou* 450001, *China*
[b)] *Research Center of Laser Fusion, China Academy of Engineering Physics, Mianyang* 621900, *China*
[c)] *Institute of Atomic and Molecular Physics, Sichuan University, Chengdu* 610065, *China*

(Received 9 October 2008; revised manuscript received 22 June 2009)

This paper applies a density functional theory (DFT) and grand canonical Monte Carlo simulations (GCMC) to investigate the physisorptions of molecular hydrogen in single-walled BC_3 nanotubes and carbon nanotubes. The DFT calculations may provide useful information about the nature of hydrogen adsorption and physisorption energies in selected adsorption sites of these two nanotubes. Furthermore, the GCMC simulations can reproduce their storage capacity by calculating the weight percentage of the adsorbed molecular hydrogen under different conditions. The present results have shown that with both computational methods, the hydrogen storage capacity of BC_3 nanotubes is superior to that of carbon nanotubes. The reasons causing different behaviour of hydrogen storage in these two nanotubes are explained by using their contour plots of electron density and charge-density difference.

Keywords: BC_3 composite nanotube, hydrogen storage, density functional theory (DFT), grand canonical Monte Carlo method (GCMC)

PACC: 6148, 7115M, 7115Q, 7125W

1. Introduction

Hydrogen has significant potential as a future energy carrier, where it can be used in efficient fuel cell technology to produce electricity particularly for mobile applications. Indeed, the U.S. Department of Energy (DOE) has established for the year 2010 a hydrogen storage target of 6% of the storage system weight for onboard automotive applications. To achieve this goal, hydrogen storage media should have large surface areas and binding energies. Carbon nanotubes (CNTs) are attractive candidates for high-capacity hydrogen storage media, particularly due to their ultrahigh surface area/weight ratio. Consequently, a great number of experimental and theoretical studies of hydrogen storage in CNTs have been reported.[1−7] However, data on the hydrogen storage capacity of CNTs are still in dispute because some experiments are not reproducible. Recent reviews[8,9] concluded that the hydrogen storage capacity of CNTs is very small (less than 1 wt %) at room temperature and moderate pressures and that CNTs are not superior to other carbon nanostructures for hydrogen storage. On the other hand, theoretical calculations yield binding energies of a single H_2 molecule on CNTs[10−13] of approximate 100 meV or less, in agreement with experimental results of the binding energies between 20 and 100 meV.[14,15] However, a thermodynamic analysis based on a comparison of the Gibbs free energies of the free gas and adsorbed hydrogen phases, using the van't Hoff equation, shows that a binding energy of about 300–400 meV/molecule would be required to meet with hydrogen storage target of DOE for viable adsorption/desorption at room temperature and moderate pressures.[10] Thus it can be seen that the hydrogen storage capacity of CNTs is hard to achieve the DOE target. Therefore, much effort has been made in finding more feasible hydrogen storage media.

The discovery of CNTs sets off a tremendous explosion for obtaining novel one-dimensional nanostructures.[16] Some nanotubes originating from hexagonal compounds, such as BC_3, have been proposed and realised experimentally.[17] Its geometries, electronic properties and possibilities for technical ap-

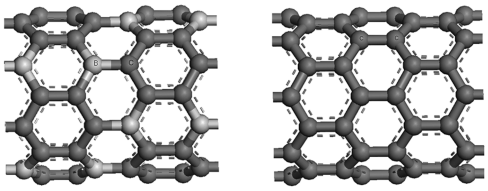
*Project supported by Henan University of Technology Foundation (Grant No. 2009BS025) and China Academy of Engineering Physics Foundation (Grant No. 2007B08008).
†Corresponding author. E-mail: liuxiuyingzx@126.com
© 2010 Chinese Physical Society and IOP Publishing Ltd

plications have been investigated theoretically.[17−19] However, to our knowledge, hydrogen adsorption in the newly proposed BC_3 nanotubes is absent. So the exploration of possible hydrogen adsorption in this nanotube is a worthy objective. Among the well-established computational techniques used to study hydrogen storage in porous materials are the density functional theory (DFT), which is a first principles quantum chemistry method and the grand canonical Monte Carlo (GCMC) simulation. The present study adopts these two computational methods to investigate the nature of adsorption and storage processes from different points of view. The aim of the DFT study is to calculate the electronic structures and the physisorption energies of molecular hydrogen on the CNTs or BC_3 nanotubes. The GCMC method is used to study the hydrogen adsorption isotherms for these two nanotubes in different conditions. The predicted hydrogen adsorption properties of BC_3 nanotubes may help experimental explorations of new nanostructured material for possible hydrogen storage medium.

2. Models and computational methods

2.1. Models

The structures of BC_3 nanotubes are classified by the chirality notation (n, m) in analogy with carbon nanotubes.[17] The optimised (8,0) structure models of carbon and BC_3 nanotubes are shown in Fig. 1.



(a) (b)

Fig. 1. The optimised structure models of the BC_3(8, 0) (a) and the C(8, 0) (b) nanotubes.

2.2. The DFT

We have performed DFT calculations by using the CASTEP code on a basis of plane waves and supercell approaches.[20] The ionic cores are replaced by ultrasoft pseudopotentials. To avoid the interaction between the tube and its periodic images, the nearest distance between two neighbouring C(8,0) or BC_3(8,0) nanotubes is no less than 10 Å. To minimise the influence of H_2–H_2 interactions along the tube axis, the computed supercells include two unit cells for both C(8,0) and BC_3(8,0). For exchange and correlation energy, we have used the local density approximation (LDA) functional of Vosko *et al.*[21] An energy cut-off of 400 eV and six k-points for sampling the one-dimensional Brillouin zone were used to optimise the geometric structures and compute the physisorption energies in the present paper.

The LDA assumes that the exchange and correlation energy is only a function of the electron density at the point of evaluation. The generalised gradient approximation (GGA), however, takes into account the gradient of the electron density at the point of evaluation. The LDA has a tendency to overestimate the binding energies.[22,23] Conversely, GGA tends to underestimate binding energies predicting a shallow or flat adsorption well.[23,24] It is well known that DFT function does not accurately describe all the characteristics of molecular interactions,[25] especially van der Waals (vdW) interactions.[24,26,27] However, in some cases, LDA has given good agreement with experimental results through fortuitous error cancellations between exchange and correlation energy approximations.[24,27,28] Note that our goal is not to predict hydrogen physisorption energies with high accuracy due to the insufficiency of the LDA exchange and correlation energy to describe the long-range dispersion interactions. However, our results at uniform levels may make comparisons of hydrogen physisorption on C and BC_3 nanotubes and provide insights to help understanding experimental findings.

The physisorption energy E_b of a H_2 molecule may measure the thermodynamic driving force for H_2 molecule adsorption on nanotubes and is given by

$$E_b = E(\text{host}) + E(H_2) - E(\text{host} + H_2), \qquad (1)$$

where E_{host} represents the total energy of the nanotube (BC_3 nanotube or CNTs), E_{H_2} is the energy of the isolated H_2 molecule, and E_{host+H_2} is the total energy of the hydrogen-nanotube system. According to this definition, the stable structure is supposed to exothermic adsorption which corresponds to $E_b > 0$.

2.3. The GCMC method

The GCMC method has been extensively used in studying equilibrium adsorption properties of sorbates, which may simulate the adsorption equilibrium

of sorbates in microporous materials with fixed chemical potential and temperature. Some important adsorption properties of sorbate molecules in the same temperature and pressure may be obtained by using GCMC method.

Lennard–Jones (LJ) potential is mainly used to study the interactions among all particles in hydrogen storage systems.[29−32] For a given pair of particles i and j with the distances r_{ij}, its LJ potential form is given by

$$\phi_{ij} = 4\varepsilon_{ij}[(\sigma_{ij}/r_{ij})^{12} - (\sigma_{ij}/r_{ij})^{6}], \tag{2}$$

where ε_{ij} and σ_{ij} are potential depth of LJ potential and length of particles, respectively.

For a system where the number of hydrogen atom, carbon atom, and boron atom are m, n and p respectively, its total potential energy is expressed as follows:

$$\begin{aligned} U = & \sum_{i_1=1}^{m-1}\sum_{i_2=i_1+1}^{m}\phi_{i_1i_2}(|\boldsymbol{r}_{i_2}-\boldsymbol{r}_{i_1}|) \\ & + \sum_{j_1=1}^{n-1}\sum_{j_2=j_1+1}^{n}\phi_{j_1j_2}(|\boldsymbol{r}_{j_2}-\boldsymbol{r}_{j_1}|) \\ & + \sum_{k_1=1}^{p-1}\sum_{k_2=k_1+1}^{p}\phi_{k_1k_2}(|\boldsymbol{r}_{k_2}-\boldsymbol{r}_{k_1}|) \\ & + \sum_{i=1}^{m}\left[\sum_{j=1}^{n}\phi_{ij}(|\boldsymbol{r}_j-\boldsymbol{r}_i|)+\sum_{k=1}^{p}\phi_{ik}(|\boldsymbol{r}_k-\boldsymbol{r}_i|)\right] \\ & + \sum_{j=1}^{n}\sum_{k=1}^{p}\phi_{jk}(|\boldsymbol{r}_k-\boldsymbol{r}_j|) \end{aligned} \tag{3}$$

where $\boldsymbol{r}_i$, $\boldsymbol{r}_j$ and $\boldsymbol{r}_k$ are position vectors of the ith H_2 molecules, the jth carbon atom and the kth boron atom respectively. The $\phi_{i_1i_2}$, $\phi_{j_1j_2}$, $\phi_{k_1k_2}$, ϕ_{ij}, ϕ_{ik} and ϕ_{jk} are interactions of hydrogen and hydrogen, carbon and carbon, boron and boron, hydrogen and carbon, hydrogen and boron, carbon and boron, respectively. Of course, if the number of some kind of atoms is zero, then the potential energy of this term is also zero.

In GCMC simulation, three types of basic operations with equal probability are generated randomly in each simulation cell: displacement, creation and deletion. The total potential energy U (before a certain operation), U' (after a certain operation) and the increment $\Delta U = U' - U$ are calculated by using Eq. (3). Then according to the assumed acceptance probabilities, this operation accepts or not. The acceptance probabilities of displacement, creation and deletion are respectively[33]

$$\min\{1, \exp[-\Delta U/k_{\mathrm{B}}T]\}, \tag{4}$$

$$\min\left\{1, \frac{V_i}{\lambda^3(N_i+1)}\exp[(\mu-\Delta U)/(k_{\mathrm{B}}T)]\right\}, \tag{5}$$

$$\min\left\{1, \frac{\lambda^3 N_i}{V_i}\exp[-(\mu+\Delta U)/(k_{\mathrm{B}}T)]\right\}, \tag{6}$$

where $\lambda = \sqrt{h^2/(2\pi m k_{\mathrm{B}}T)}$, h is Planck constant, m is the mass of H_2 molecule, T is temperature, μ is the chemical potential, V_i is the volume of the ith subspace, and N_i is the number of H_2 molecules in the ith subspace. The above operations are repeated until systems reach equilibrium. In the simulations, periodic boundary conditions are used; 1×10^6 steps are used for simulation lengths in order to equilibrate the system and 1×10^7 steps to calculate the chemical potentials.

3. Results and discussion

3.1. Optimized structures of BC_3 and carbon nanotubes

The BC_3(8,0) and the C(8,0) nanotubes were fully relaxed in supercells, and the optimised structure parameters are listed in Table 1. As shown in this table, the C–C bond lengths in BC_3 and CNTs are comparable, i.e. 1.410 Å and 1.409 Å, respectively, which agree well with the experimental values of 1.415 Å,[34] or 1.41 Å.[35] The B–C bond length in BC_3 nanotubes is 1.548 Å, which is also in agreement with the calculated values 1.55 Å.[36] Therefore, our optimised results are reasonable. As a consequence of these individual bond lengths, the diameter D and the tubular length l in the BC_3(8,0) nanotubes are also larger than those in the C(8, 0) nanotubes (Table 1).

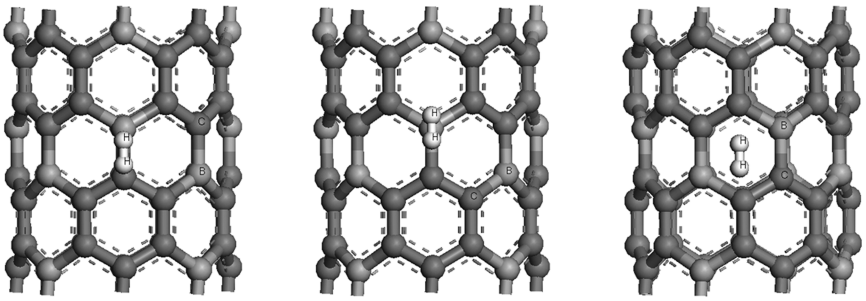
Table 1. Diametre D, supercell length l and average bond length d for C(8,0) and BC_3(8,0) nanotubes after geometric optimisations (1 Å = 0.1 nm).

nanotube	D/Å	l/Å	d/Å
BC_3(8,0)	6.506	8.864	$d_{C-C} = 1.410$, $d_{C-B} = 1.548$
C(8,0)	6.263	8.520	$d_{C-C} = 1.409$

3.2. The DFT study of hydrogen physisorptions in BC_3 and carbon nanotubes

We have studied the physisorptions of molecular hydrogen in BC_3(8,0) and C(8,0) nanotubes. Three adsorption sites were studied with the axis of H_2 molecule whose orientation is parallel to the nanotube

surface. For C(8,0) nanotube, the adsorption sites correspond to site A, above C–C bond; site B, on top of a C atom; and site C, the centre of a hexagon. Likewise, for BC_3(8,0) nanotube, the corresponding adsorption sites are site A, above B–C bond; site B, on top of a B atom; and site C, the centre of a hexagon. The three adsorption sites in the BC_3(8,0) are given in Fig. 2.



(a) (b) (c)

Fig. 2. The adsorption sites of a H_2 molecule in BC_3(8,0) nanotube: (a) site A: above B–C bond; (b) site B: on top of a B atom; (c) site C: the centre of a hexagon.

The physisorption energies of H_2 adsorbed on the BC_3 and CNTs are displayed in Table 2 along with the equilibrium distance between the hydrogen molecule's centre of mass and the nanotube wall. As shown in this table, although the physisorption energies have no significant differences, they are slightly dependent on the locations of an H_2 molecule. The most stable configuration is site C, whose physisorption energies and equilibrium distances are 116.48 meV and 2.7 Å for the BC_3(8,0) nanotube and 78.3 meV and 2.9 Å for the C(8,0) nanotube, respectively. Cabria *et al.*[37] recently studied the hydrogen adsorption on the C(7,7) nanotube by using DFT with exchange and correlation energy of LDA, and reported physisorption energy and equilibrium distance with H_2 molecule located at the centre of a hexagon outside the nanotube are 100 meV and 2.5 Å respectively. Furthermore, Henwood and Carey[38] also studied the hydrogen physisorption on the C(9,0) and the C(10,0) nanotubes by using DFT with both LDA and GGA exchange and correlation energy. For the same adsorption site with ours, the physisorption energies and equilibrium distances are 79.2 meV and 2.7 Å for the C(10,0) nanotube and 79.75 meV and 2.7 Å for the C(9,0) nanotube, respectively, which are also in agreement with ours. Thus the prediction of physisorption energies for the BC_3(8,0) nanotubes are believable. We may also see that from Table 2, all physisorption energies are larger for hydrogen adsorbed on BC_3 nanotubes in comparing with the physisorption energies of hydrogen physisorbed to CNTs. And the physisorption energies of BC_3(8,0) nanotube are an average of 40.15 meV larger than those of C(8,0) nanotube. Therefore, it is indicated that BC_3 nanotube is energetically more favourable than CNT for hydrogen storage.

Table 2. Physisorption energies E_b (in meV/molecule) and equilibrium distances D_{eq} (in Å) for the different adsorption sites in the C(8,0) and the BC_3(8,0) nanotubes. The equilibrium distances D_{eq} (in Å) are measured from the nanotube wall to the mass centre of an H_2 molecule.

adsorption site	C(8,0)		BC_3(8,0)		
	D_{eq}	E_b	D_{eq}	E_b	ΔE_b
A	3.0	71.87	2.8	113.74	41.87
B	2.9	73.59	2.8	113.81	40.22
C	2.9	78.03	2.7	116.48	38.45

In order to analysing the reasons why the hydrogen storage capacity of BC_3 nanotube is superior to CNT, firstly, we have computed the charge-density differences of BC_3 and CNTs. Because charge-density difference may illustrate the interaction of a H_2 molecule with nanotubes, especially it may show how the electronic structure is distorted by the two molecule's proximity to one another. The charge-density difference is defined by

$$\Delta\rho = \rho_{(\text{host}+H_2)} - (\rho_{(H_2)} + \rho_{(\text{host})}), \qquad (7)$$

where ρ_{host} is the charge density of the nanotube (BC_3 nanotube or CNTs), $\rho_{(H_2)}$ is the charge density of the isolated H_2 molecule, and $\rho_{(\text{host}+H_2)}$ is the total charge density of the hydrogen-nanotube system.

For the adsorption site C, the contour plots of charge-density difference $\Delta\rho$ for the C(8,0) and the

BC_3(8,0) nanotubes are plotted in Fig. 3. As shown in this figure, significant charge redistribution in the C(8,0) nanotube is clearly seen, which leads to the concentration of electronic charge between CNT and H_2 molecule, but there is no charge deviation between them. However, for the BC_3(8,0) nanotube, there are some charge deviation of H_2 molecule towards nanotubes, thus it shows a certain extent properties of chemisorptions. Therefore, the interaction of BC_3 nanotube with H_2 molecule is stronger than that of CNT with H_2 molecule. This may also be explained from the electron densities of these two nanotubes. The contour plots of electron densities of these two nanotubes are plotted in Fig. 4, which correspond to the cross section in a yz plane along z axis of the nanotubes. The white regions and the black one denote high electron density areas and low electron density areas, respectively. The overlap indicates covalent bonding between atoms. For the C(8,0) nanotube, we may see clearly the conjugated bonds of carbon atoms (Fig. 4(a)). The BC_3(8,0) nanotube also shows this structure, however, due to the lower electronegativeness of B atom compared with C atom and forming an electron-deficient structure, it displays the lopsided densities characteristic including a certain extent of ionic B–C bonding (Fig. 4(b)), and the electron densities near B atoms are much lower than those near C atoms. Therefore, the electron-deficient BC_3 nanotubes adsorbed H_2 molecule more effectively than CNTs.



Fig. 3. Contour plots of charge-density difference of the adsorption site C for the C(8,0) (a) and the BC_3(8,0) (b) nanotubes which correspond to the cross section (xy-plane) along x axis through the centre of mass of H_2 molecule.

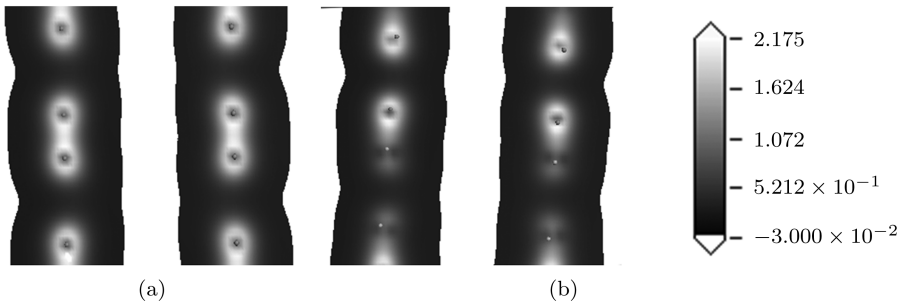


Fig. 4. Contour plots of the electron densities for the C(8,0) (a) and the BC_3(8,0) (b) nanotubes which correspond to the cross-sections (yz-plane) along the axis (z direction) of the nanotubes.

For the sites A and B, the contour plots of charge-density difference for the C(8,0) and the BC_3(8,0) nanotubes are plotted in Figs. 5 and 6, respectively. Together with Fig. 3, we can see that the interaction of

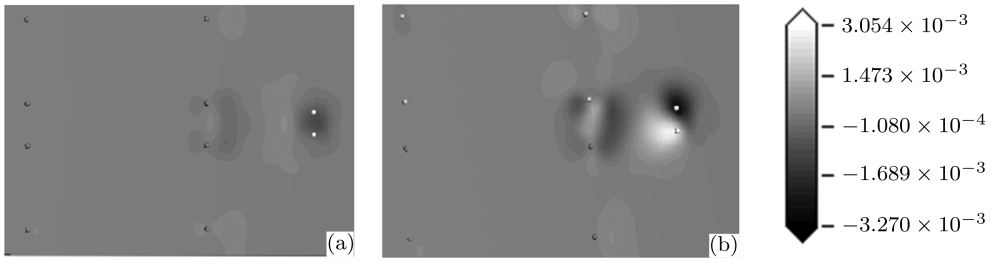


Fig. 5. Contour plots of charge-density difference of the adsorption site A for the C(8,0) (a) and the BC_3(8,0) (b) nanotubes which correspond to the cross section (xz-plane) through the axis of H_2 molecule.

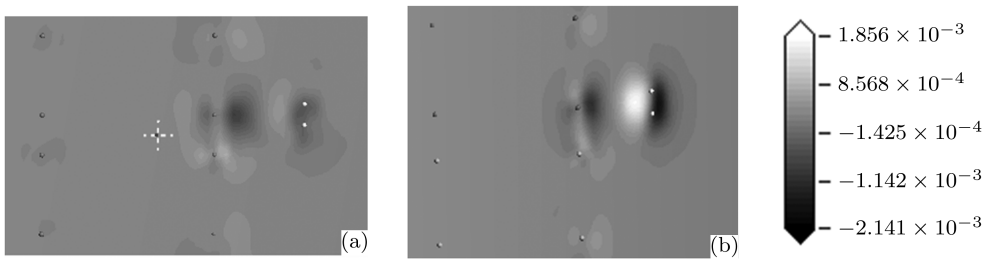


Fig. 6. Contour plots of charge-density difference of the adsorption site B for the C(8,0) (a) and the BC_3(8,0) (b) nanotubes which correspond to the cross section (xz-plane) through the axis of H_2 molecule.

BC_3 nanotube with H_2 molecule is stronger than that of CNT with H_2 molecule. This is mainly because of the existence of more electronegative B atom and the asymmetric structure of 6 MR. Due to the asymmetric structure of 6 MR, the contributions of B atom to physisorption energies of different adsorption sites are slightly different. As a consequence, the physisorption energy E_b is largest in site C, intermediate in site B, smallest in site A (Table 2).

3.3. The GCMC study of hydrogen physisorptions in BC_3 and CNTs

In a given temperature, we may obtain the relationship between hydrogen physisorption amounts and pressure by varying pressure of the system, i.e. adsorption isotherms. Firstly, in order to validate correctness and accuracy of our calculated results, the computed adsorption isotherms of the C(7,7) nanotube in a broad range of temperature (77 K–300 K) and pressure (0–10 MPa), shown in Fig. 7, were compared with those results which were investigated by Cabria *et al.*[37] using quantum-thermodynamic model method. As shown in this figure, our calculated hydrogen adsorption amounts are 0.59 wt% and 2.38 wt% at 300 K and 77 K respectively with a pressure of 10 MPa, which are in agreement with 0.6 wt% and 2.5 wt% in Ref. [37]. Thus, our results are believable.

Then we studied the adsorption isotherms of the BC_3(8,0) and the C(8,0) as a function of the pressure for several different temperatures using GCMC method, as shown in Fig. 8. We can see that the adsorption amounts increase and saturate with increasing pressure, which are in agreement with experiments on porous carbons.[39,40] And the adsorption amounts correspondingly increase with decreasing temperature. However, there is a maximal adsorption limit. For the BC_3(8,0) nanotube, the adsorption limit is 1.602 wt%, which may be reached at 10 MPa and 200 K, 0.5 MPa and 77 K, respectively; however, this limit is not reached at room temperature 300 K, which is the temperature of interest. Comparably, the C(8,0) nanotube will reach its adsorption limit 0.520 wt% at 5 MPa and 200 K, 0.2 MPa and 77 K, respectively; and this limit is also not reached at 300 K.

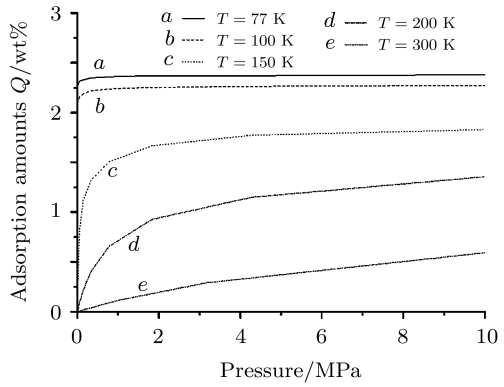


Fig. 7. The adsorption isotherms of the C(7,7) nanotube in a range of temperatures from 77 K to 300 K.

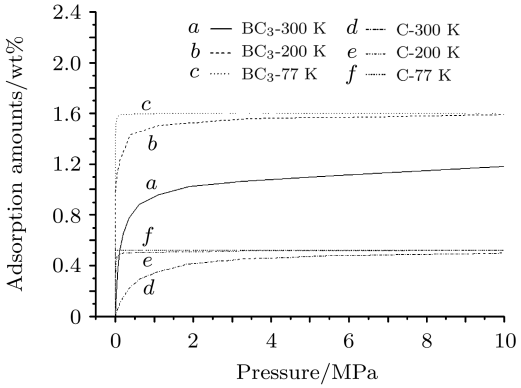


Fig. 8. The adsorption isotherms of the BC3(8,0) and the C(8,0) nanotubes at 300 K, 200 K and 77 K.

Differently, the adsorption amounts of the

BC_3(8,0) are larger than those of the C(8,0) for all temperatures examined. Concretely, the adsorption amounts of the former are 1.182 wt%, 1.589 wt% and 1.602 wt% at 300 K, 200 K and 77 K respectively with a pressure of 10 MPa, while the adsorption amounts of the latter correspond to 0.497 wt%, 0.520 wt% and 0.520 wt%, respectively. Furthermore, the difference of the adsorption amounts of 0.023 wt% between 200 K and 300 K with a pressure of 10 MPa for the C(8,0) nanotube is much smaller than 0.407 wt% for the BC_3(8,0) nanotube. This suggests that the increased adsorption amounts of CNT are small when temperature lowers; however, for the BC_3 nanotube, there is a noticeable increment of adsorption amounts with the decrease of temperature from room temperature to a lower temperature before reaching its adsorption limit, and the adsorption amounts are no longer increased after reaching its adsorption limit even when temperature is further lowered.

To sum up, the GCMC results are consistent with those obtained using DFT. Both these results indicate that BC_3 nanotube has a higher hydrogen storage capacity, thus it may be a better hydrogen storage medium than CNTs.

4. Conclusions

We have studied the interactions of molecular hydrogen with BC_3 and CNTs using DFT and GCMC methods, respectively. The DFT calculations show that the adsorption of H_2 in BC_3 nanotubes is more favourable and energetical than CNTs. And the GCMC studied results illustrate quantitatively that the adsorption amounts of H_2 in BC_3 nanotubes are larger than those in CNTs. Essentially, these two results are consistent, which show that the hydrogen adsorption capacity of BC_3 nanotubes is stronger than that of CNTs. The results help to understand hydrogen adsorption properties of these two nanotubes and explore new hydrogen storage candidates experimentally.

Acknowledgements

The authors acknowledge fruitful discussions with Ge Fang-fang.

References

[1] Dillon A C and Heben M J 2001 *Appl. Phys.* A **72** 133
[2] Ding R G, Lu G Q, Yan Z F and Wilson M A 2001 *J. Nanosci. Nanotechnol.* **1** 7
[3] Meregalli V and Parrinello M 2001 *Appl. Phys.* A **72** 143
[4] Hirscher M and Becher M 2003 *J. Nanosci. Nanotechnol.* **3** 3
[5] Liu C and Cheng H M 2005 *J. Phys.* D **38** R231
[6] Chen D, Yu B H, Wang C L and Gao T 2007 *Chin. Phys.* **16** 2056
[7] Liu X Y, Wang C Y, Tang Y J, Sun W G, Wu W D, Zhang H Q, Liu M, Yuan L and Xu J J 2009 *Acta Phys. Sin.* **58** 1126 (in Chinese)
[8] Züttel A 2003 *Mater. Today* **9** 24
[9] Orimo S, Züttel A, Schlapbach L, Majer G, Fukunaga T and Fujii H 2003 *J. Appl. Crystallogr.* **356** 716
[10] Li J, Furuta T, Goto H, Ohashi T, Fujiwara Y and Yip S 2003 *J. Chem. Phys.* **119** 2376
[11] Froudakis G E 2001 *Nano. Lett.* **1** 531
[12] Arellano J S, Molina L M, Rubio A, López M J and Alonso J A 2002 *J. Chem. Phys.* **117** 2281
[13] Cabria I, López M J and Alonso J A 2005 *Europ. Phys. J.* D **34** 279
[14] Brown C M, Yildirim T, Newmann D A, Heben M J, Gennett T, Dillon A C, Alleman J L and Fischer J E 2000 *Chem. Phys. Lett.* **329** 311
[15] Narehood D G, Pearce J V, Eklund P C, Sokol P E, Lechner R E, Pieper J, Copley J R D and Cook J C 2003 *Phys. Rev.* B **67** 205409
[16] Iijima S 1991 *Nature* **354** 56
[17] Miyamoto Y, Rubio A, Louie S G and Cohen M L 1994 *Phys. Rev.* B **50** 18360
[18] Kim Y H, Chang K J and Louie S G 2001 *Phys. Rev.* B **63** 205408
[19] Kim Y H, Sim H S and Chang K J 2001 *Current Appl. Phys.* **1** 39
[20] Accelrys Inc. 2001 *Material Studio CASTEP* (San Diego: Accelrys Inc.)
[21] Vosko S H, Wilk L and Nusair M 1980 *Can. J. Phys.* **58** 1200
[22] Han S S and Lee H M 2004 *Carbon* **42** 2169
[23] Giannozzi P, Car R and Scoles G 2003 *J. Chem. Phys.* **118** 1003
[24] Lazic P, Crljen Ž, Brako R and Gumhalter B 2005 *Phys. Rev.* B **72** 245407
[25] van den Berg A W C, Bromley S T, Wojdel J C and Jansen J C 2005 *Phys. Rev.* B **72** 155428
[26] Khantha M, Cordero N A, Molina L M, Alonso J A and Girifalco L A 2004 *Phys. Rev.* B **70** 125422
[27] Du A J and Smith S C 2005 *Nanotechnol.* **16** 2118
[28] Rigamonti S and Proetto C R 2006 *Phys. Rev.* B **73** 235319
[29] Williams K A and Eklund P C 2000 *Chem. Phys. Lett.* **320** 352

[30] Cheng J R, Yuan X H, Zhao L, Huang D C, Zhao M, Dai L and Ding R 2004 *Carbon* **42** 2019
[31] Kang J W and Hwang H J 2004 *J. Phys.: Condens. Matter* **6** 3901
[32] Darkrim F and Levesque D 1998 *J. Chem. Phys.* **19** 4981
[33] Frenkel D and Smit B 2001 *Understanding Molecular Simulation From Algorithms to Applications* (Orlando: Academic)
[34] Ubbelohde A R 1960 *Graphite and its Crystal Compounds* (Oxford: Clarendon) p5
[35] Pierson H O 1993 *Handbook of Carbon, Graphite, Diamond, and Fullerenes: Properties, Processing and Applications* (New Jersey: Noyes) p45
[36] Zhou Z, Zhao J J, Gao X P, Chen Z F, Yan J, Schleyer P R and Morinaga M 2005 *Chem. Mater.* **17** 992
[37] Cabria I, López M J and Alonso J A 2008 *J. Chem. Phys.* **128** 144704
[38] Henwood D and Carey J D 2007 *Phys. Rev.* B **75** 245413
[39] Gogotsi Y, Dash R K, Yushin G, Yildirim T, Laudisio G and Fischer J E 2005 *J. Am. Chem. Soc.* **127** 16006
[40] Jordá-Beneyto M, Suárez-García F, Lozano-Castelló D, Cazorla-Amorós D and Linares-Solano A 2007 *Carbon* **45** 293